The Structure of Butyl Carbamate and of Its Water Complex in the Gas Phase

Pablo Pinacho,[a†] *Juan Carlos López,*[*a] *Zbigniew Kisiel,*[b] *and Susana Blanco.*[a*]

[a] Departamento de Química Física y Química Inorgánica, IU CINQUIMA, Facultad de Ciencias, Universidad de Valladolid, E-47011 Valladolid, Spain. [b] Institute of Physics, Polish Academy of Sciences, Warsaw, Poland.

KEYWORDS. Rotational Spectroscopy, Molecular Structure, Hydrogen Bonded Complexes.

ABSTRACT. The structure of butyl carbamate and of its complex with water generated in a supersonic expansion has been characterized by Fourier transform microwave spectroscopy. Up to 13 low-energy conformations of the monomer have been predicted which differ in the relative orientation of the butyl chain and the amide group. However, only three conformations have been observed experimentally. The remaining low energy conformers are expected to interconvert into the observed rotamers through collisional relaxation processes in the supersonic jet. The values of the C-O-C_α-C_β dihedral angle observed for the two most stable conformers of butyl carbamate, with extended configurations, can be directly correlated with the values of this angle in the two experimentally observed conformers of the shorter-chain molecule, ethyl carbamate. The less stable form shows a weak C-H···O=C intramolecular hydrogen bond from the terminal methyl group to the carbamate C=O group, stabilizing a folded configuration. For the most stable butyl carbamate monomer the complex with one molecule of water has been observed. In that complex the water molecule attaches to the amide group in a cyclic arrangement using two hydrogen bonds. The results indicate that water does not substantially alter the conformational behavior of butyl carbamate.

Introduction

Carbamates, frequently called urethanes, are a large family of organic compounds present in many biomolecules playing a key role in medicinal chemistry.[1,2] Carbamate compounds are derived from carbamic acid, in which one, two or three hydrogen atoms have been substituted by an organic chain. In this way, when the hydrogen of the carboxylic group is substituted, the carbamate is defined as an ester-derivative of an amide, and thus it presents some of the features of the peptide bond. One important aspect of the carbamates is their ability to regulate the formation of inter- or intramolecular interactions with enzymes or receptors.[2] Carbamates are observed in biochemistry as protein or amino acid residues and also as intermediates in several processes.[3] In addition, they are implicated in Calvin cycle in the vegetal photosynthesis so can be also related to global warming.[4] Besides their use as insecticides[5,6] and their importance for pharmacotherapy in medicinal chemistry, some carbamates are also important in industry, especially for polymer synthesis.[7]

In order to understand the properties of carbamates and relate them to their chemical or biological behavior it is essential to analyze their possible conformations and relative stabilities. Also, it is important to study the proton donor or acceptor character which is important to characterize their reactivity[8,9] or to know how some properties, such as electron density, can vary when the substituents change or when the carbamate interacts with other molecules.[10]

The study of carbamates in the gas phase can provide valuable information regarding structural disposition preferences and conformational distribution. When the number of carbon atoms in the carbamate side chain increases, more low-energy conformations arise. Some of them could be stabilized by long-range intramolecular interactions between the aliphatic chain and the amide group. Thus, the study of long-chain carbamates could contribute to the understanding of the possibilities of formation of inter- *vs*. intra-molecular interactions. They can also serve to model the interactions between polar and non-polar groups. Only a few carbamates have so far been studied in the gas phase, and only those with "short" lateral chains. Methyl carbamate has probably been the carbamate which has received most attention since it is a candidate precursor of biological molecules in the interstellar medium. Its structure has been thoroughly characterized by microwave,[11-14] IR spectroscopy,[15] or X-ray crystallography.[16] A second member of the family, ethyl carbamate, has also been characterized by microwave,[17,18] IR spectroscopy,[19] and X-ray crystallography.[20]

In contrast, no similar study has so far been performed for longer chain carbamates. In this work we aimed to investigate the structure of butyl carbamate (Bcb) (see Scheme 1) and of its complex with water by taking advantage of the power of high-resolution microwave spectroscopy. Such experiments have presently been carried out at conditions of supersonic expansion where it is possible to study isolated molecules at very low temperature, when their properties are not affected by solvent or self-aggregation effects. We have also detected in the supersonic jet and analyzed the 1:1 complex formed between Bcb and water.

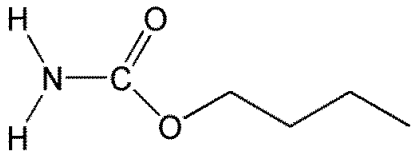

Scheme 1. Butyl carbamate ($C_5H_{11}NO_2$).

Experimental and theoretical methods

Butyl carbamate ($C_5H_{11}NO_2$), a white crystalline solid with melting point of *ca.* 55°C, was purchased and used without further purification (98%). The microwave spectrum (2-8 GHz) of butyl carbamate was first recorded in a chirped-pulse Fourier transform spectrometer (CP-FTMW).[21,22] The sample was held in a stainless steel heated nozzle at approximately 90-100°C in order to increase its population in the gas phase. The vapor of butyl carbamate was mixed with Ar carrier gas, which for the investigation of the microsolvated complex was previously seeded with water vapor, at a stagnation pressure of 1.6 bars. A supersonic jet was generated by pulsing the gas mixture (for *ca.* 900 μs) through a small diameter nozzle (0.8 mm) into the high vacuum chamber. A chirped pulse of *ca.* 5 μs covering a 2 GHz bandwidth was used for sample polarization. The molecular emission FID signal was recorded for about 10 μs. In this instrument the frequency measurement accuracy is better than 15 kHz, with resolution power better than 30 kHz. Refined measurements between 5-18 GHz were done in two narrow band Fourier transform, Fabry-Perot cavity microwave spectrometers (MB-FTMW), in Valladolid[23] and at the Institute of Physics in Warsaw.[24] The experimental conditions of pressure and temperature were similar to the ones described above. In these instruments, a short microwave pulse of *ca.* 1-5 μs is emitted to polarize the sample at a discrete frequency, and a narrow spectral segment is recorded. However, the frequency measurement accuracy is better than 3 kHz, with resolution of

better than 10 kHz, which allowed complete resolution of the hyperfine structure due to ^{14}N nuclear quadrupole coupling. A comparison between the chirped-pulse and the cavity instruments for the same transition is shown in Figure 1. The intensity of the spectra was not sufficient to observe any isotopologues in natural abundance. The spectrum of the complex using a mixture of isotopically enriched $H_2{}^{18}O$ with $H_2{}^{16}O$ in proportion of 1:3 was recorded in the MB-FTMW spectrometer in Valladolid. Several transitions were measured for the monoisotopically substituted ^{18}O complex to determine its rotational constants.

The conformational space of butyl carbamate was investigated by exploring the dihedral angles d_1=∠N-C-O-C$_\alpha$, d_2=∠C-O-C$_\alpha$-C$_\beta$, d_3=∠O-C$_\alpha$-O$_\beta$-C$_\gamma$ and d_4=∠C$_\alpha$-C$_\beta$-C$_\gamma$-C$_\delta$ (see Figure 2) giving rise to the different stable structures shown in Figure S1. Geometry optimizations[25] were first done using the DFT hybrid functional B3LYP[26-28] combined with GD3[29] empirical dispersion correction and the 6-311++G(d,p)[30] basis set. Further *ab initio* optimizations at the MP2/6-311++G(d,p)[31] and MP2/aug-cc-pVDZ[32] levels of theory. In all cases the harmonic approximation was used to calculate the Gibbs energy and vibrational frequencies, confirming that all predicted configurations were true minima. The conformers were initially labelled from I to XIII according to their Gibbs energies at MP2/6-311++G(d,p) (see Tables S1-S3). When analyzing the different forms of butyl carbamate two facts should be taken into account. First, the amino group is predicted to be in a slightly pyramidal configuration, so for each conformer there is a corresponding non-equivalent inverted form, with the exception of conformer III, which is predicted to have two equivalent forms. Fortunately, the energy difference between the inverted NH_2 forms is very small, with a predicted barrier to planarity of around 10 cm^{-1} with respect to the high-energy form. In this case, it can be expected that ground vibrational state of the inversion vibration is above the barrier in all cases, with an effectively nearly planar structure for the amino group. Second, butyl carbamate shows transient chirality so that each form given in Figure S1 has a non-superimposable mirror image conformer, again with the exception of form III. It is noted that transient enantiomers in each pair have the same energy and rotational parameters being thus indistinguishable with conventional rotational spectroscopy. For that reason we have also adopted an alternative notation to identify easily the different conformers by using four successive letters to describe the values of the d_1, d_2, d_3 and d_4 dihedral angles. The labels T, G^+, G^-, A^+ or A^- were used to denote the antiperiplanar (T, ~180º), synclinal (G^+, ~60º; G^-, -60º) or anticlinal (A^+, ~120º; A^-, ~-120º), configurations respectively according to

conventional Newman projections. In Tables S1-S3 for each of the I-XIII forms they are given the two four-letter labeling corresponding to each of the two equivalent mirror image forms.

Finally, the structures for complexes with water were predicted for monomers I and IV taking into account that, as has been demonstrated in other systems,[9,33,34] complex formation as controlled by a kinetic mechanism, occurs mainly from the conformers present with appreciable concentration in the jet. As described below this occur only for forms I and IV of butyl carbamate. The corresponding water complexes of those forms were calculated at the MP2/6-311++G(d,p) level of theory (see Figure S2 and Table S3) based on the complexes observed in previous works for microsolvation of amides.[8,10,22,33,35,36]

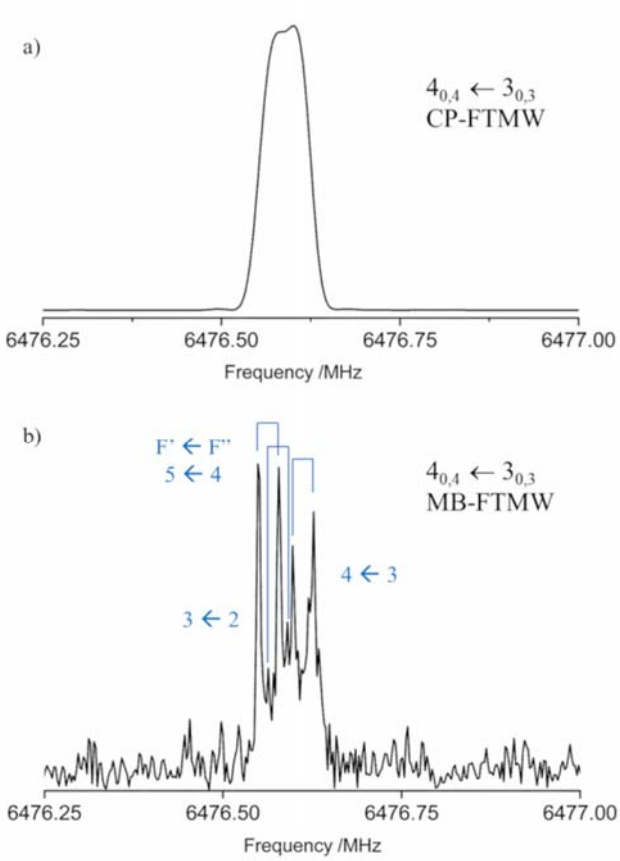

Figure 1. The $4_{0,4} \leftarrow 3_{0,3}$ rotational transition for the butyl carbamate I monomer showing the difference in the resolution for the hyperfine structure (F′←F′′ transitions) as measured in a) CP-FTMW, or in b) MB-FMTW. In the lower spectrum each transition appears as a doublet due to the instrumental Doppler effect.

Results and discussion

Microwave spectra

The predicted rotational constants, dipole moment components and quadrupole coupling constants were used to simulate the spectra for the monomers. In general, the predicted dipole moment components are sufficiently large to lead to observable *a*, *b* and *c*-type spectra, with μ_b the most prominent dipole moment component for the majority of the monomers (see Tables S1-S3). The analysis of the experimental *b*-type patterns in the CP-FTMW spectrum resulted in the assignment of two species which were matched with conformers I and IV (see Figure 2). After this identification, *a* and *c*-type transitions were also measured and added to the fit for both forms. Once the lines belonging to conformers I and IV were removed it was possible to observe μ_a R-branch groups of lines which allowed assignment of the complex between monomer I and one molecule of water (see Figure 2). A new cleaning of the CP-FTMW spectrum from the complex spectral lines allowed us to assign a weak series of Q-branch *b*-type lines from their frequency and ^{14}N quadrupole coupling hyperfine structure patterns. The parameters determined from the Q-branch lines ((A-C)/2 = 1050.3 MHz and κ=-0.819) correlate with the calculated parameters of conformers VIII and XII. The observation of very weak R-branch, *a*-, *b*- and *c*-type transitions seems to indicate that the observed conformer is probably VIII (see Figure 2), since form XII has a μ_a electric dipole moment component predicted to be close to zero. Lines in the 5-18 GHz frequency range were measured in the MB-FTMW spectrometers so as to determine the more precise values for the rotational parameters and to resolve the ^{14}N hyperfine structure (see Figure 1). The final fits (see Table 1 for the monomers and Table 2 for the complex) were made using an A-reduced semirigid asymmetric rotor Hamiltonian in the I^r representation supplemented by a quadrupole coupling term.[37-39] For the $H_2{}^{18}O$ isotopologue the fit was made by fixing the centrifugal distortion and quadrupole coupling constants to the values determined for the parent species (see Table 2). The experimental frequencies for all the observed species are collected in Tables S5-S9.

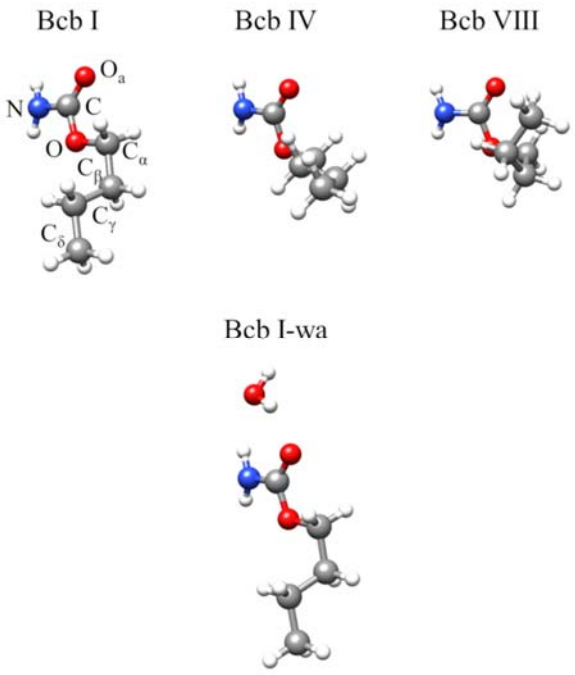

Figure 2. Experimentally observed monomers for butyl carbamate and the 1:1 butylcarbamate and water complex.

Table 1. Experimental rotational parameters for the Bcb I, Bcb IV and Bcb VIII monomers compared to *ab initio* (MP2/6-311++G(d,p)).

	Bcb I		Bcb IV		Bcb VIII	
Parameters[a]	Expt.	*ab initio*	Expt.	*ab initio*	Expt.	
A /MHz	5172.37967(31)[b]	5107.35	5408.12217(52)	5231.20	3230.0583 (11)	3160.53
B /MHz	850.195022(77)	856.82	827.679134(71)	840.67	1319.07575(61)	1351.92
C /MHz	771.611551(74)	775.37	793.827259(64)	805.65	1129.43719(59)	1155.91
P_{aa} /uÅ^2	575.842738(41)	571.34	576.892790(37)	565.92	337.06547(23)	325.57
P_{bb} /uÅ^2	79.122839(41)	80.45	59.743203(37)	61.37	110.39554(23)	111.65
P_{cc} /uÅ^2	18.584413(41)	18.50	33.704946(37)	35.24	46.06575(23)	48.26
Δ_J /kHz	0.13555(27)	0.142	0.14017(57)	0.135	0.668(28)	0.634
Δ_{JK} /kHz	-2.4651(40)	-2.64	-1.7600(80)	-1.73	-0.596(22)	0.059
Δ_K /kHz	24.310(35)	25.4	24.290(65)	21.2	4.27(29)	3.01
δ_J /kHz	0.00832(11)	0.0774	0.016237(61)	0.0162	0.1234(12)	0.105
δ_K /kHz	0.798(29)	0.816	[0.]	1.49	1.558(34)	1.577
3/2(χ_{aa}) /MHz	2.5041(31)	2.83	1.8438(79)	2.69	0.6494(82)	1.63
¼(χ_{bb}-χ_{cc}) /MHz	1.39568(68)	1.21	0.90683(98)	1.08	0.6505(20)	0.85
n	306/108		163/56		110/35	
σ /kHz	3.8		4.5		7.5	

[a] A, B and C are rotational constants, $P_{\alpha\alpha}$ (α = a, b or c) are planar moments of inertia; these are derived from the moments of inertia I_α as for example P_{cc} = (I_a+I_b-I_c)/2, Δ_J, Δ_{JK}, Δ_K, δ_J and δ_K are quartic centrifugal distortion constants, χ_{aa}, χ_{bb}, χ_{cc}, are nuclear quadrupole coupling tensor diagonal elements for the ^{14}N atom. n is the number of quadrupole hyperfine components fitted. After the slash is the number of rotational transitions fitted. σ is the rms deviation of the fit. [b] Standard errors are given in parentheses in units of the last digit. [c] Parameters in square brackets were kept fixed.

Table 2. Experimental rotational parameters for the parent and $^{18}O_w$ species of the Bcb I-wa complex compared to *ab initio* (MP2/6-311++G(d,p)).

	Bcb I-wa				Bcb I-wa		
Parameters[a]	Parent	^{18}O	*ab initio*	Parameter	Parent	^{18}O	*ab initio*
A /MHz	4882.90(22)[b]	4870.95(57)	4953.99	P_{aa} /uÅ^2	976.8921(48)	1015.117(12)	973.62
B /MHz	504.92384(62)	486.23283(10)	507.93	P_{bb} /uÅ^2	79.4904(48)	79.494(12)	80.66
C /MHz	478.40531(61)	461.69722(10)	479.36	P_{cc} /uÅ^2	24.0093(48)	24.259(12)	21.36
3/2(χ_{aa}) /MHz	1.858(47)	[1.858]	2.20	Δ_J /kHz	0.05381(43)	[0.05381][c]	0.0048
¼(χ_{bb}-χ_{cc}) /MHz	1.495(30)	[1.495]	1.25	Δ_{JK} /kHz	-2.677(14)	[-2.677]	-2.164
n	111/39	45/15		Δ_K /kHz	[0.]	[0.]	53.1
σ /kHz	2.4	2.3		δ_J /kHz	-0.00294(28)	[-0.00294]	-0.0015
				δ_K /kHz	1.71(29)	[1.71]	0.582

[a] See Table 1 for definitions.

Structure

The comparison of the experimental rotational constants with those calculated at the different levels of theory for all the predicted conformers (see Tables S1-S3) indicates that the observed rotamers should be correlated with forms I, IV and VIII. The degree of agreement between experiment and theory is similar for the different levels of theory. Table 1 compares the observed parameters with those calculated at MP2/6-311++G(d,p) level for these conformers. The agreement for the rotational constants is better than 1% for conformer I and 3% for conformers IV and VIII. In all cases, there is a somewhat better agreement for constants *B* and *C*. Further confirmation can be obtained from the values of the planar moments of inertia P_{aa} , P_{bb} and P_{cc}, giving the mass extension away from the *bc, ac* and *bc* planes, respectively. The agreement for the quadrupole coupling constants is worst because these constants are very sensitive to the configuration on the amino group and probably the experimental ground state constants, which are vibrationally averaged, do not reflect the NH_2 configuration calculated at the minima. This is illustrated in Figure S4 where the predicted dependence of the quadrupole coupling constants with the NH_2 inversion coordinate is depicted. The experimentally observed values are approximately reproduced for a value of the dihedral angle ∠HNCO ~ 5º. In any case, the good agreement between observed and calculated parameters allows us to take the optimized structures for conformers I, IV and VIII as reasonable descriptions of the structures of the observed butyl carbamate forms.

In butyl carbamate, the rotational constants and planar moments give also an indication of the relative orientation of the amide group and the butyl chain. Forms I (κ = -0.964) and VI (κ = -0.985) are nearly prolate asymmetric tops indicating extended configurations which have

comparable rotational constants. In those conformers the molecule does not adopt a totally planar skeleton arrangement, as reflected by their P_{cc} values (18.5844 u·Å^2 and 33.7049 u·Å^2, respectively). The planar, linearly extended skeleton configuration corresponds to the predicted structure Bcb III (P_{cc} = 6.4 u·Å^2), which has not been observed experimentally. Conformer VIII, on the other hand is less prolate (κ = -0.819), has a smaller value of the *A* rotational constant and a relatively high P_{cc} value (46.065 u·Å^2), suggesting a folded structure. These conclusions can be understood by taking into account the values of the d_1 – d_4 dihedral angles since the configuration of I is defined as T–T–G$^+$–T, that of IV as T–G$^+$–T–T, and that of VIII as T–A$^+$–G$^-$G$^-$.

It is interesting to remark that the two most stable forms of Bcb have the same configuration for the dihedral angles d_1 and d_2 as the two observed conformers of ethyl carbamate, Ecb I (T–T) and Ecb II (T–G$^+$).[18] The values of the d_2 =C-O-Cα-Cβ dihedral angle for Bcb I is *ca.* 180 degrees, while for Bcb IV it has a value close to 80 degrees. Those values are in good agreement with the same dihedral angle for the experimental structures observed for Ecb I (T–T) and Ecb II (T–G$^+$) (see Table 3). In that work, the special stability of Ecb II was attributed to a weak intramolecular interaction between the hydrogen on Cβ and the carbonyl oxygen. Based on the *ab initio* predicted C-H···O distances, interactions of this type could also be present in forms IV and VIII but also in other butyl carbamate conformers (see Table S4). The plausible C-H···O interactions have been investigated using Quantum Theory of "atoms in molecules" (QTAIM)[40,41] to locate bond paths (BP) and bond critical points (BCP). The results for the observed conformers are summarized in Figure 3 where BPs and BCPs are shown and weak C-H···O interactions were found only for conformer VIII. Estimation of the interaction energy is also given in the figure. In addition a non-covalent interaction (NCI) analysis[42] has been performed in order to visualize the weak adduct interactions. In the NCI plot (see Figure 3), intermolecular interactions are visualized as isosurfaces whose color codes indicate the strengths of attractive or repulsive interactions.

Table 3. Theoretical dihedral angle for the observed conformers of butyl carbamate and ethyl carbamate.

	Bcb I	Bcb IV	Ecb I[a]	Ecb II[a]
C-O-Cα-Cβ /°	177.4	80.2	179.8	82.5

[a] from reference 18.

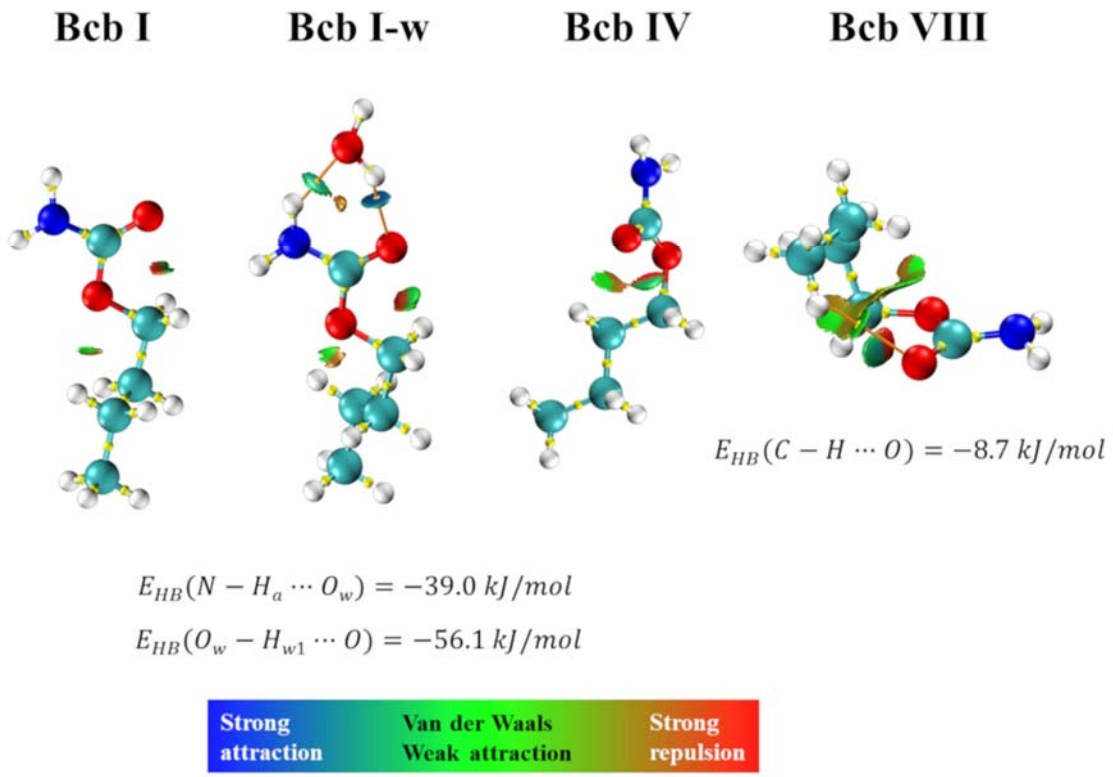

Figure 3. Bond paths (orange), ring and bond critical points (yellow) combined with NCI isosurfaces with S=0.5 for the observed conformers of butyl carbamate and butyl carbamate – water complex. The strength of the C-H···O interaction estimated from the electron potential density (V(r)/2) at the BCPs is given for form VIII and those for O-H···O and N-H···O for the complex.

The rotational parameters of the species observed in the presence of water also show good agreement with those predicted for the monohydrate complex of butyl carbamate (see Table 2). The degree of agreement is at 1.4, 0.6 and 0.2 % for A, B and C rotational constants, respectively. The observation of the ^{18}O water complex isotopologue (see Table 2) gives additional structure information allowing us to locate the position of the water molecule. Analysis of the changes of the planar moments with isotopic substitution is an excellent starting point to analyze the structure of the complex. P_{bb} has identical values (within experimental error) in the parent and in the ^{18}O species, indicating that the oxygen atom lies in the *ac* plane (see Figures 4 and S3). In the same way the small change observed for P_{cc} indicates that the water

oxygen is close to the *ab* plane. These observations combined with the fact that only P_{aa} shows significant changes upon substitution indicates that the water oxygen lies practically on the *a* axis with very low values of the *b* and *c* principal coordinates (see Figures 4 and S3).

Two different approaches have been used to explore the structure of the Bcb I-wa complex by exploiting the information obtained from the ^{18}O isotopologue. The first method, r_0 structure,[43] gives a partial effective structure from a least-square fit of certain distances and angles to reproduce the experimental moments of inertia in the ground vibrational state.[44] For the Bcb I-wa complex the best r_0 structure has been obtained by fitting the $O_a\cdots H_{w1}$ distance and the C-$O_a\cdots H_{w1}$ angle and fixing the rest of the molecular parameters to the *ab initio* values. The second method, the r_s substitution structure, is based on the changes occurring in the moments of inertia due to monoisotopic substitution. By solving the Kraitchman equations[45] this method gives the absolute values of the coordinates for the substituted atom in the principal inertial axis system of the parent molecule. The signs for the coordinates have to be assigned from other structures, such as r_0 or r_e. The uncertainties in the coordinates of the ^{18}O atom have been quoted following the Costain rule.[46] The results for r_e, r_0 and r_s structures are summarized in Figure 4.

The intermolecular interactions established between butyl carbamate and water are similar to those previously reported for monohydrated complexes of molecules bearing the amide group.[8,10,22,33,35,36] The water molecule interacts with the polar end of butyl carbamate closing a 6 member cycle through the formation C-$O_a\cdots H_{w1}$-$O_w\cdots H_f$-N hydrogen bond network (see Figures 4 and S3). In this complex, both butyl carbamate and water are acting simultaneously as hydrogen donor and acceptor. The experimental value of P_{cc} increases from the monomer (18.5844 u·Å^2) to the monohydrated complex (24.0093 u·Å^2), supporting the notion that water interacts in this typical directional manner with the amide group (lone pair of the oxygen to the amino H). Since the latter is out of the *ab* inertial plane it makes the non-planar disposition of the water molecule more noticeable (see Figures 4 and S3).

In the theoretical calculation for the Bcb I-wa complex, the dihedral angles of the butyl chain have similar values as in the monomer. This indicates that the water molecule interacts solely with the amide and the carbonyl groups and does not substantially affect the structure of the butyl carbamate backbone.

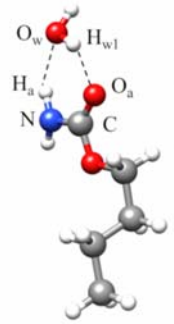

Parameter	r_0	r_e
$r(H_{w1}\cdots O_a)$ /Å	1.720(8)	1.77
$\angle(H_{w1}\cdots O_a\text{-}C)$ /°	188(2)	180

	Atom	*a*	*b*	*c*
$\lvert r_s \rvert$ /Å		4.39882(51)	0.044(50)	0.3629(63)
r_0 /Å	O_w	4.37718(81)	0.052(22)	-0.4194(47)
r_e /Å		4.415	0.015	-0.045

Figure 4. The Bcb I-wa complex showing atom labelling with the partial effective r_0 structure, compared to the calculated r_e structure, and with comparison of the O_w coordinates for r_s, r_0 and r_e structures.

Conformational interconversion

Despite the presence of unassigned lines in the experimental spectrum, no other monomers were observed, although there are other low energy conformers predicted, with energies even lower than for the observed forms, as in the case for Bcb II conformer. The non-observation of those forms could be explained by invoking conformational interconversion through energy barriers lower than *ca.* 400 cm^{-1} by collisional relaxation in the supersonic jet.[47,48] Some interconversion barriers have been obtained at the B3LYP/6-311G level of theory by calculating the bidimensional potential energy surfaces by scanning the dihedral angles d_1 – d_4. In figure 5a the surface corresponding to the relaxed scan of angles d_2 (C-O-C_α-C_β) and d_3 (O-C_α-C_β-C_γ) in steps of 15 degrees, while keeping d_1 and d_4 angles fixed to T configurations. In this energy surface it is possible to identify the minima of conformers I to VIII. The possible potential energy function paths for their interconversion can be envisaged by following the valleys along the d_2 (C-O-C_α-C_β) dihedral angle connecting forms I, II and VI or III and IV. These paths are illustrated in figures 5b and 5c showing the one-dimensional functions calculated at B3LYP-D3/6-311++G(d,p). Figure 5d shows the d_2 dihedral angle path connecting forms V, VII and VIII. The figures show how conformers II and VI can interconvert into I, III into IV and V or VII into VIII, by overcoming low barriers in consistency with the observation of forms I, IV and VIII only. The

fact that these three conformers are observed indicate that these should correspond to the most stable forms within each series of conformers, for example form I is more stable than form II, even if the minimum for the latter is predicted to be the global minimum at the levels of theory used. The inclusion of the water molecule does not substantially change the shape of the potential function and the energy barriers as shown in figure 5b.

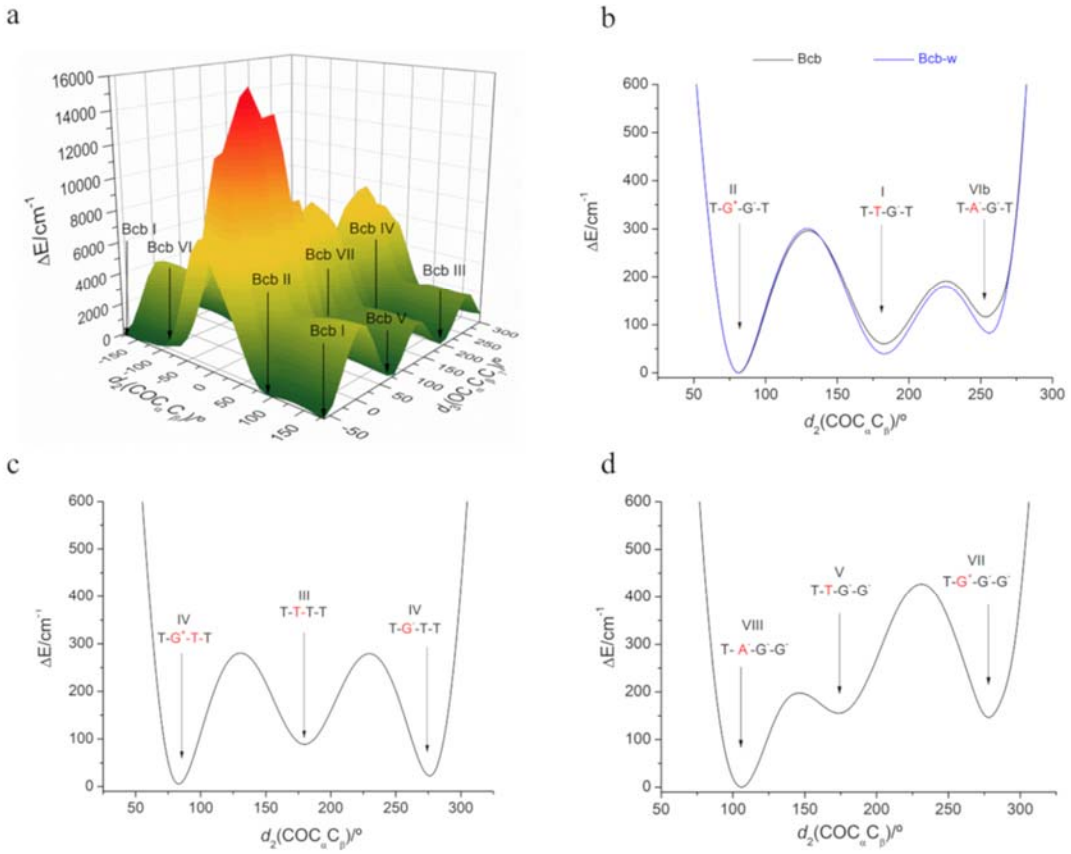

Figure 5. a) Bi-dimensional potential energy surface for the relaxed scan of the d_2 (C-O-Cα-Cβ) and d_3 (O-Cα-CβCγ) dihedral angles at the B3LYP-d3/6-311G level of theory showing the minima corresponding to forms I to VII of butyl carbamate (see Figure S1 and Tables S1-S2). b-d) One-dimensional potential energy functions (B3LYP-D3/6-311++G(d,p)) for the relaxed scan of the d_2 (C-O-Cα-Cβ) dihedral angle, for three different configurations of the d_3-d_4 dihedral angles (b: G^+-T; c: T-T; d: G^- -G^-) showing possible paths for conformational relaxation to the I, IV and VIII conformers through low energy barriers. In b, VIb refers to conformer VI with the amino group inverted.

Conclusions

The structure of butyl carbamate has been studied in the gas phase by high-resolution microwave spectroscopy. Thirteen different conformations have been predicted to be low-energy minima on the potential energy surface of butyl carbamate. The only significant change between all of them is the different relative orientation of the butyl chain. From all of the possible rotamers, only three have been observed experimentally. The two most stable forms present extended structures in correspondence with the monomers observed for the related molecule, ethyl carbamate. This correspondence is reflected in similar values of the C-O-C_α-C_β dihedral angle. The less stable conformer VIII presents a folded structure reinforced by a weak C-H···O intramolecular interaction from the terminal methyl group to the carbamate C=O group, which contributes to its stabilization. A similar interaction was invoked for ethyl carbamate in order to explain the unexpected low energy of the second most stable conformation.[18] The lack of observation of the remaining structures, even those with low energy, could be explained by the existence of collisional relaxation processes taking place in the supersonic expansion which interconvert them into the detected conformers through rotation around the O-C_α bond. Exploration of the potential energy function along this coordinate show low interconversion barriers. In addition, the monohydrated complex of the most stable form of butyl carbamate has been observed. This complex is stabilized by a C-O_a···H_w-O_w···H-N hydrogen bond network. These types of interactions have been reported for similar molecules containing the amide group.[8,10,22,33,35,36] In the complex, the structure of the butyl carbamate molecule seems to remain essentially unchanged.

ASSOCIATED CONTENT

The Supporting Information includes figures for all the predicted conformations of the monomer and monohydrated complex, their predicted rotational constants and the list of experimental frequencies measured for all the assigned species. This material is available free of charge via the Internet at http://pubs.acs.org.

AUTHOR INFORMATION

Corresponding Author

*E-mail: jclopez@qf.uva.es. *E-mail: sblanco@qf.uva.es.

Present Addresses

†Deutsches Elektronen-Synchrotron DESY, Notkestraße 85, 22607 Hamburg, Germany.

Author Contributions

The manuscript was written through contributions of all authors. All authors have given approval to the final version of the manuscript.

Funding Sources

Ministerio de Economia y Competitividad (Grant CTQ 2016–75253-P)

ACKNOWLEDGMENT

PPM, JCL and SB acknowledge the Ministerio de Economía y Competitividad (Grant CTQ 2016-75253-P) for financial support and to the University of Valladolid (UVa) for a predoctoral mobility grant. PPM acknowledges the University of Valladolid for the mobility grant (Ayudas para estancias breves en el desarrollo de Tesis Doctorales de la UVa) and ZK for his kind hospitality in Warsaw.

REFERENCES

[1] Abraham, D. J., Rotella, D. P. Burger´s medicinal chemistry, drug discovery and development, 7th edition, Wiley, Hoboken, 2010.

[2] Ghosh, A. K., Brindisi, M. “Organic Carbamates in Drug Design and Medicinal Chemistry” *J. Med. Chem.*, **2015**, 58, 2895–2940.

[3] Bartoschek, S., Vorholt, J. A., Thauer, R. K., Geierstanger, B. H., Griesinger, C., "N-Carboxymethanofuran (carbamate) formation from methanofuran and CO_2 in methanogenic archaea: Thermodynamics and kinetics of the spontaneous reaction", *Eur. J. Biochem.*, **2001**, 267, 3130-3138.

[4] Berg, J. M., Tymoczko. J. L., Stryer, L. Biochemistry 7th Edition, W. H. Freeman, New York, 2012.

[5] Tiwari, B., Kharwar, S., Tiwari, D. N. in Cyanobacteria: Chap. 15 Pesticides and Rice Agriculture. Elsevier, 2019.

[6] Fukuto, T. R. "Mechanism of Action of Organophosphorus and Carbamate Insecticides" *Environ. Health Perspect.*, **1990**, 87, 245–254.

[7] Heyn, R. H., Jacobs, I. C., R. H. "Synthesis of Aromatic Carbamates from CO_2: Implications for the Polyurethane Industry" *Adv. Inorg. Chem.*, **2014**, 66, 83–115.

[8] Blanco, S., Pinacho, P., López, J. C. "Hydrogen-Bond Cooperativity in Formamide$_2$-Water: A Model for Water Mediated Interactions" *Angew. Chem. Int. Ed.*, **2016**, 128, 9477–9481.

[9] López, J. C., Macario, A., Blanco, S. "Conformational equilibria in *o*-anisic acid and its monohydrated complex: the prevalence of the *trans*-COOH form" *Phys. Chem. Chem. Phys.*, **2019**, 21, 6844-6850.

[10] Blanco, S., Pinacho, P., López, J. C. "Structure and Dynamics in Formamide-$(H_2O)_3$: A Water Pentamer Analogue" *J. Phys. Chem. Lett.*, **2017**, 8, 6060–6066.

[11] Marstokk, K. M., Møllendal, H. "Microwave Spectrum, Conformation, Barrier to Internal Rotation, ^{14}N Quadrupole Coupling Constants, Dipole Moment and Quantum Chemical Calculations for Methyl Carbamate" *Acta Chem. Scan.*, **1999**, 53, 79–84.

[12] Bakri, B., Demaison, J., Kleiner, I., Margulès, L., Mollendal, H., Petitprez, D., Wlodarczak, G. "Rotational Spectrum, Hyperfine Structure, and Internal Rotation of Methyl Carbamate" *J. Mol. Spectrosc.*, **2002**, 215, 312–316.

[13] Groner, P., Winnewisser, M., Medvedev, R., De Lucia, F. C., Herbst, E. Sastry, K. V. L. N. "The Millimeter- and Submillimeter-Wave Spectrum of Methyl Carbamate [$CH_3OC(:O)NH_2$]" *ApJS*, **2007**, 169, 28–36.

[14] Ilyushin, V., Alekseev, E., Demaison, J., Kleiner, I. "The Ground and First Excited Torsional States of Methyl Carbamate" *J. Mol. Spectrosc.*, **2006**, 240, 127–132.

[15] Kydd, R. A., Rauk, A. "The Equilibrium Geometry of Methyl Carbamate" *J. Mol. Struct.*, **1981**, 77, 227-238.

[16] Sepehrnia, B., Ruble, J. R., Jeffrey, G. A. "Methyl Carbamate" *Acta Crystallogr.*, **1987**, C43, 249–251.

[17] Marstokk, K. M., Møllendal, H. "Microwave Spectrum, Conformational Equilibrium and Quantum Chemical Calculations of Urethane (Ethyl Carbamate)" *Acta Chem. Scand.*, **1999**, 53, 329–334.

[18] Goubet, M., Motiyenko, R. A., Réal, F., Margulès, L., Huet, T. R., Asselin, P., Soulard, P., Krasnicki, A., Kisiel, Z., Alekseev, E. A. "Influence of the Geometry of a Hydrogen Bond on Conformational Stability: A Theoretical and Experimental Study of Ethyl Carbamate" *Phys. Chem. Chem. Phys.*, **2009**, 11, 1719–1728.

[19] Furer, V. L. “Hydrogen Bonding in Ethyl Carbamate Studied by IR Spectroscopy” *J. Mol. Struct.*, **1998**, 449, 53–59.

[20] Bracher, B. H., Small, R. W. H. “The Crystal Structure of Ethyl Carbamate” *Acta Crystallogr.*, **1967**, 23, 410–418.

[21] Brown, G. G., Dian, B. C., Douglass, K. O., Geyer, S. M., Shipman, S. T., Pate, B. H. “A Broadband Fourier Transform Microwave Spectrometer Based on Chirped Pulse Excitation” *Rev. Sci. Instrum.*, **2008**, 79, 053103.

[22] Pinacho, P., Blanco, S., López, J. C. “The complete conformational panorama of formanilide–water complexes: the role of water as a conformational switch” *Phys. Chem. Chem. Phys.*, **2019**, 21, 2177–2185.

[23] Alonso, J. L., Lorenzo, F. J., López, J. C., Lesarri, A., Mata, S., Dreizler, H. “Construction of a Molecular Beam Fourier Transform Microwave Spectrometer Used to Study the 2,5-Dihydrofuran-Argon Van Der Waals Complex” *Chem. Phys.*, **1997**, 218, 267–275.

[24] Kisiel, Z., Kosarzewski, J., Pszczółkowski, L. “Nuclear Quadrupole Coupling Tensor of CH_2Cl_2: Comparison of Quadrupolar and Structural Angles in Methylene Halides” *Acta Phys. Pol. A*, **1997**, 92, 507–516.

[25] Gaussian 09, Revision D.01, Frisch M. J., Trucks G. W., Schlegel H. B., Scuseria G. E., Robb M. A., Cheeseman J. R., Scalmani G., Barone V., Petersson G. A., Nakatsuji H., Li X., Caricato M., Marenich A., Bloino J., Janesko B. G., Gomperts R., Mennucci B., Hratchian H. P., Ortiz J. V., Izmaylov A. F., Sonnenberg J. L., Williams-Young D., Ding F., Lipparini F., Egidi F., Goings J., Peng B., Petrone A., Henderson T., Ranasinghe D., Zakrzewski V. G., Gao J., Rega N., Zheng G., Liang W., Hada M., Ehara M., Toyota K., Fukuda R., Hasegawa J., Ishida M., Nakajima T., Honda Y., Kitao O., Nakai H., Vreven T., Throssell K., Montgomery, Jr. J. A., Peralta J. E., Ogliaro F., Bearpark M., Heyd J. J., Brothers E., Kudin K. N., Staroverov V. N., Keith T., Kobayashi R., Normand J., Raghavachari K., Rendell A., Burant J. C., Iyengar S. S., Tomasi J., Cossi M., Millam J. M., Klene M., Adamo C., Cammi R., Ochterski J. W., Martin R. L., Morokuma K., Farkas O., Foresman J. B., Fox D. J., Gaussian, Inc., Wallingford CT, 2016.

[26] Lee, C., Yang, W., Parr, R. G. “Development of the Colle-Salvetti Correlation-Energy Formula into a Functional of the Electron Density” Phys. Rev. B, 1988, 37, 785–789.

[27] Becke, A. D. “Density-Functional Thermochemistry. III. The Role of Exact Exchange” J. Chem. Phys., 1993, 98, 5648–5652.

[28] Vosko, S. H., Wilk, L., Nusair, M. “Accurate Spin-Dependent Electron Liquid Correlation Energies for Local Spin Density Calculations: a Critical Analysis” Can. J. Phys., 1980, 58, 1200–1211.

[29] Grimme, S., Antony, J., Ehrlich, S., Krieg, H. “A Consistent and Accurate Ab Initio Parametrization of Density Functional Dispersion Correction (DFT-D) for the 94 Elements H-Pu” J. Chem. Phys., 2010, 132, 154101.

[30] Ditchfield, R., Hehre, W. J., Pople, J. A. "Self-Consistent Molecular-Orbital Methods. IX. An Extended Gaussian-Type Basis for Molecular-Orbital Studies of Organic Molecules" *J. Chem. Phys.*, **1971**, 54, 724–728.

[31] Møller, C., Plesset, M. S. "Note on an Approximation Treatment for Many-Electron Systems" *Phys. Rev.*, **1934**, 46, 618–622.

[32] Dunning Jr., T. H. "Gaussian basis sets for use in correlated molecular calculations. I. The atoms boron through neon and hydrogen" *J. Chem. Phys.*, **1989**, 90, 1007–1023.

[33] Caminati, W., López, J. C., Blanco, S., Mata, S., Alonso, J. L. "How water links to *cis* and *trans* peptidic groups: the rotational spectrum of N-methylformamide-water" *Phys. Chem. Chem. Phys.,* **2010**, 12, 10230–10234.

[34] Macario, A., Blanco, S., Thomas, J., Xu, Y., López, J. C. "Competition between intra- and inter-molecular hydrogen bonding: *o*-anisic acid···formic acid heterodimer", *Chem. Eur. J.*, **2019**, in press.

[35] Held, A., Pratt, D. W. "Hydrogen Bonding in Water Complexes. Structures of 2-Pyridone-H_2O and 2-Pyrididone-$(H_2O)_2$ in Their S_0 and S_1 Electronic States" *J. Am. Chem. Soc.*, **1993**, 115, 9708–9717.

[36] Blanco, S., López, J. C., Lesarri, A., Alonso, J. L. "Microsolvation of Formamide: A Rotational Study" *J. Am. Chem. Soc.*, **2006**, 128, 12111–12121.

[37] Gordy, W., Cook, R. L. Microwave Molecular Spectra, Wiley-Interscience, New York, 1984.

[38] Watson, J. K. G. in Vibrational Spectra and Structure a Series of Advances, Vol 6 ed. J. R. Durig, Elsevier, New York, 1977, pp. 1–89.

[39] Pickett, H. M. "The Fitting and Prediction of Vibrational-Rotation Spectra with Spin Interaction" *J. Mol. Spectrosc.*, **1991**, 148, 371–377.

[40] Bader, R. F. W. "A Quantum Theory of Molecular Structure and Its Applications" Chem. Rev. **1991**, 91, 893–928.

[41] Lu, T.; Chen, F. "Multiwfn: A Multifunctional Wavefunction Analyzer". *J. Comput. Chem*. **2012**, 33, 580–592.

[42] Johnson, E. R.; Keinan, S.; Mori-Sánchez, P.; Contreras-García, J.; Cohen, A. J.; Yang, W. "Revealing Noncovalent Interactions." *J. Am. Chem. Soc.* **2010**, 132 (18), 6498–6506.

[43] Rudolph, H. D. "Contribution to the Systematics of r_0-Derived Molecular Structure Determinations from Rotational Parameters" *Struct. Chem.*, **1991**, 2, 581–588.

[44] Kisiel, Z. "Least-Squares Mass-Dependence Molecular Structures for Selected Weakly Bound Intermolecular Clusters" *J. Mol. Spectrosc.*, **2003**, 218, 58–67.

[45] Kraitchman, J. “Determination of Molecular Structure from Microwave Spectroscopic Data” *Am. J. Phys.*, **1953**, 21, 17–24.

[46] Costain, C. C. “Further Comments on the Accuracy of r_s Substitution Structures” *Trans. Am. Crystallogr. Assoc.*, **1966**, 2, 157–164.

[47] Ruoff, R. S., Klots, T. D., Emilsson, T., Gutowsky, H. S. “Relaxation of Conformers and Isomers in Seeded Supersonic Jets of Inert Gases” *J. Chem. Phys.*, **1990**, 93, 3142–3150.

[48] Godfrey, P. D., Brown, R. D., Rodgers, F. M. “The Missing Conformers of Glycine and Alanine: Relaxation in seeded Supersonic Jets” *J. Mol. Struct.*, **1996**, 376, 65–81.